Interactive Pipeline for Mandible Reconstruction Surgery Planning using Fibula Free Flap

Sylvain Leclerc[1*], Bianca Jansen Van Rensburg[1], Thibault De Villèle[1], Marie De Boutray[1,2], Nabil Zemiti[1], Noura Faraj[1]

[1]LIRMM, Université Montpellier, CNRS, Montpellier, France.
[2]Department of ENT, Neck Surgery and Maxillofacial Surgery, Gui de Chauliac University Hospital, Montpellier, France.

*Corresponding author(s). E-mail(s): sylvain.leclerc@achline.fr;

Abstract

Purpose Mandible reconstruction surgery using fibula free flap is a long and expensive process requiring extensive surgical experience. Indeed, the planning stage, mandible shaping, and therefore osteotomy positioning on the fibula is tedious, often done by hand and can take months. This delay is unacceptable when mandible deterioration is caused by a time-sensitive disease such as cancer. In this paper, we propose an interactive pipeline for an easy-to-use and time-efficient surgical planning tool tailored to be used directly by the surgeon.
Methods From CT scans of patient's mandible and fibula, we propose to register a cutting structure to the mandible and to segment and mesh the fibula, then, respecting anatomical constraints (mandible curvature, flap size, vessel preservation,...), we generate a surgery plan. Next, in a 3D interactive environment, the surgeon can intuitively shape the mandible by cutting, moving, and modifying bone fragments non-destructively. This stage allows surgeons to express their expertise, the resulting cutting plane positions are then sent to a robot serving as a cutting guide for the surgery.
Results We demonstrate the efficiency of our method through patient specific surgery planning for two different pathologic cases. We show our results are comparable to a commercial solution away from cutting guides design.
Conclusion Our proposed pipeline allows for a patient specific precise planning and to cut down the preoperative planning phase of the mandible reconstruction surgery from days to minutes.

Keywords: Mandible reconstruction, Fibula free flap, Interactive system, 3D modeling, Interactive volume rendering, Computed tomography segmentation.

Statements and Declarations

This work has been partially supported by the French National Agency for Research (Agence Nationale pour la Recherche, ANR) within the Investissements d'Avenir Program (Labex CAMI, ANR-11-LABX0004, Labex NUMEV, ANR-10-LABX-20, and the ROBOTEX 2.0 (Grants ROBOTEX ANR-10-EQPX-44-01 and TIRREX ANR-21-ESRE-0015))

1 Introduction

Today, mandible reconstruction surgery is a long and costly process requiring extensive surgical training. The best option currently available in the case of mandible deterioration is to reconstruct the mandible using bone and tissue taken from another part of the patient's body [1]. The most suitable graft is the Fibula Free Flap (FFF) [2]: using segments of the fibula bone accompanied by the surrounding tissues, as well as a thin blood vessel: the pedicle. It is attached along the bone, ensuring its vascularisation. The FFF is preferred for two main reasons: the fibula contains sufficient bone material to reconstruct the mandible, and its partial removal does not impair the patient's walking ability. The main challenge emerging from this choice is that the straight fibula flap needs to be cut into small angled segments, using a surgical saw, to reproduce the curved mandible morphology (Figure 1).

1.1 Background

The success of the mandible reconstruction using a FFF depends on the quality of the flap design and positioning on the mandible defect. It thus implies performing adapted cuts (osteotomies) which respect some medical constraints (detailed in 1.2). This result in a FFF mimicking the patient mandible's shape. Hence, careful planning of mandible and fibula osteotomies is required. Among the different planning methods developed by surgeons two are the most common. The first is based on the use of stereolithographic guides which are designed virtually, printed, and accompanied by titanium plates custom-made to fit the patient's anatomy [3]. These patient-specific

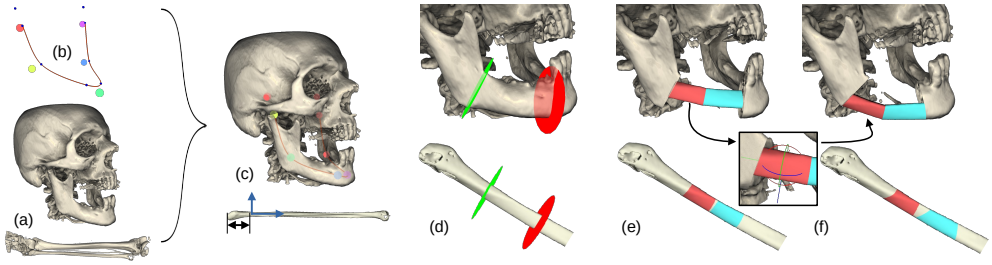

Fig. 1: Overview of the proposed pipeline. Starting from a patient head and lower body CT scan (a), a reference curve (b) is registered onto the patient head, and the fibula is segmented (c). Cutting planes are placed on the mandible (d) to make a first surgery plan (e) which can be refined using manual adjustments (f).

guides and plates are usually manufactured far from the hospital by external companies, one of them being Materialise (Leuven, Belgium). A second method is an in-house 3D-printing planning of the surgery. For this, surgeons print 3D models of the patient's mandible and fibula, and then plan the surgery by cutting the 3D printed models [4]. The main drawbacks of these methods are their price, manufacturing time, and/or the fact that they are time-consuming to produce with possible imprecision. The delay before the surgery could be dire when mandible deterioration is caused by a time-sensitive disease such as cancer. in those cases, the mandible's shape could have changed by the time the surgery is performed. Virtual planning of the operation from computed tomography images has already proven to be a viable method to reduce planning and operating times [5]. Existing planning methods [4] require the generation of patient specific fibula and mandible surface meshes. Mesh generation methods [6, 7], require the segmentation of regions of interest which is a difficult task. While possible for the fibula, it is especially for the mandible since the data includes patient-specific anatomy singularities associated with their pathology (missing regions, spongy bones, metal artifact interference, unusual topologies...), artifacts inherent to the imaging method, and lack of measurable separation between the bone of interest and the other bones (e.g. mandible's condyles and skull). Therefore, segmentation is mostly done manually by the surgeon [8] which is tedious and time-consuming, or done in an expensive proprietary solution, one of the most used being Mimics® (Materialise, Leuven, Belgium) [9]. To cope with this difficulty, a deep learning based method was proposed for mandible segmentation [10]. Nonetheless, while such methods perform well for standard pathologies, it fails for extreme cases. Moreover, mandible segmentation based approach inevitably results in the loss of crucial information contained in the image's gray levels providing valuable details about the bone's internal structure, density, and porosity needed by the surgeon to make the best reconstruction, effectively removing all cancerous area, placing screws in dense enough areas.

Current state-of-the-art methods for mandible reconstruction surgery planning present several limitations. First, for this specific surgery it is crucial to let the surgeon the more freedom possible, because of the variety of cases. For example, patients may require a higher reconstruction to allow a future tooth graft, while older patient may benefit from a lower, more robust placement. The surgeon also have to consider the aesthetic of the reconstruction, without compromising the functional role of the mandible. However, proposed methods do not let the surgeons have direct control over the planning, and thus to express their expertise. This could be due to overly complex steps, such as manual segmentation, or unintuitive user interfaces more than often requiring help of a trained third person. Fibula segmentation is a simpler task because, since the only information that we need from the fibula is the outside shape, the structure of the leg's bones being well known and, in our cases, not pathological. Second, proposed methods are time-consuming, with significant delays caused by the need for external companies to produce cutting guides and custom plates. Finally, deep learning approaches, while effective in many cases, do not guarantee success for extreme or unusual cases, making them unreliable in critical scenarios.

To overcomes these issues, we propose a pipeline for a patient specific mandible reconstruction surgery planning, illustrated in Figure 1, that drastically cuts the cost

and reduces time needed to plan a surgery by giving the total control over the planning to the surgeon, while being simple to use. To do so, we eliminate the need for external segmentation and any pre-processing of the data. We work directly with the raw patient's CT scans, preserving all available information. We designed the process to be as simple as possible for the surgeon by providing a good automatic planning, then we give the surgeon a total control over the procedure, allowing for easy adjustments to fit the operation to the specific needs of each patient.

The goal of our surgical planning tool is to compute cutting planes for mandible resection and FFF segmentation, using patients 3D CT scans of the mandible and lower body while respecting medical constraints. We propose to use guides for cutting planes' trajectories on both mandible and fibula. We first place a cutting curve in the patient's mandible image using a semi-automatic non-rigid registration. For the fibula, we propose a bone specific segmentation method, allowing surgeons to quickly and reliably segment the bone. Then the cutting structure is placed in the middle of the resulting mesh.

1.2 Medical constraints

During surgery, four main medical constraints have to be respected. First, a **minimum distance** constraint aiming at maintaining the integrity of the fibula and not to impair the ankle's stability. A minimum distance of 6 cm of fibula bone has to be preserved on the distal part of the fibula (*i.e.* distal malleolus). Second, the **offset** constraint, the gap between two fibula fragments must be large enough to allow the saw to pass without kinking the pedicle. We denote this distance to be 1 mm. Third, a **minimum size** constraint, when reconstructing the mandible, the length of each fibula segment must be $>$ 2.5 cm to ensure the vascularization of bone fragments. A **torsion** constraint is imposed since the pedicle (attached to the FFF) should not be twisted in order to ensure flap vascularization, and thus its engraftment on the mandible. This implies that FFF fragments have to be rotated as little as possible in relation to one another while being placed in the mandible.

2 Proposed method

Our method can be decomposed into four main steps:

- **Initialization:** A cutting guide - a curve - is registered to the CT scan of the patient's mandible, the fibula is segmented and meshed by the surgeon in our application (Section 2.1).
- **Mandible and Fibula resection:** The surgeon selects the deteriorated section of the mandible, after which our system computes the corresponding regions of the fibula to extract (Section 2.4).
- **Cutting planes estimation:** We define the *polyline*: a new structure based on the curve which allows the cutting planes to be automatically positioned and orientated, while respecting prescribed medical constraints. The proposed reconstruction is computed by replacing a selected deteriorated section of the mandible with resulting fibula segments (Section 2.4).

- **User refinements:** Using a set of interactive manipulators, the surgeon is given the option to make adjustments leveraging his/her expertise to meet mechanical and aesthetic requirements (Section 2.5).

The resulting cutting plane coordinates are transferred to a robot serving as a cutting guide designed to assist the surgeon [11]. Note that during the entire pipeline, the visual results (fibula bone fragments along with a iso-surface rendering of input CT) are updated in real-time to enable interactive editing and feedback.

2.1 Registration

Reference curve The main goal of our pipeline is the placement of cutting planes in the patient's mandible and fibula. To do so, we use as a Catmull-Rom interpolation curve [12] noted $\mathcal{C}_{\text{ref}}$. It is defined using a set of control points $\Phi = \{\phi_i\} \subset \mathbb{R}^3$ through which the curve passes exactly. This curve represents the theoretical optimal path for the fibula fragments, hence for the cutting planes (Figure 2), through the bone. $\mathcal{C}_{\text{ref}}(t)$ at $t \in [0, 1]$ defines the position of the cutting plane and the tangent at t its orientation. The control points of this curve are defined relatively to a set of anatomical landmarks $\mathcal{L}_{\text{ref}}$ on $\mathcal{I}_{\text{ref}}$, that have been placed on a healthy mandible, with the help of a specialized surgeon. These points are used to deform the curve from the generic model, to the patient's anatomy.

Mandible curve registration To perform a non-rigid registration of the reference curve on the patient CT we define a set of matching reference frames on both side and compute the new control points using a weighted sum of the resulting transformations. First, the surgeon places anatomical landmarks $\mathcal{L}_{\text{pat}}$, corresponding to $\mathcal{L}_{\text{ref}}$ on the patient's mandible CT scan $\mathcal{I}_{\text{pat}}$ as illustrated in Figure 3.
Then we define a frame for each landmark (in both $\mathcal{L}_{\text{i}}^{\text{ref}}$ and $\mathcal{L}_{\text{i}}^{\text{pat}}$) noted $\mathcal{F}_{\text{i}} = (\mathbf{x}_i, \mathbf{y}_i, \mathbf{z}_i)$. Note that, since the only goal is to compute the transformation T_i between $\mathcal{L}_{\text{i}}^{\text{ref}}$ and $\mathcal{L}_{\text{i}}^{\text{pat}}$, we only need the frames vectors $(\mathbf{x}_i, \mathbf{y}_i, \mathbf{z}_i)$ to be defined consistently relative to each other. We choose to use $\mathbf{x}_i = \mathcal{L}_{\text{i+1}} - \mathcal{L}_{\text{i}}$, then with $\mathcal{L} = \sum_{j=0}^{n} \mathcal{L}_{\text{j}}/n$ the average of the landmarks positions $\mathbf{y}_i = \mathcal{L} - \mathcal{L}_{\text{i}}$ with n being the number of landmark. Then we compute the last vector $\mathbf{z}_i$ as a vector orthogonal to x_i and y_i, $\mathbf{z}_i = \mathbf{x}_i \wedge \mathbf{y}_i$. Finally $\mathbf{x}_i, \mathbf{y}_i, \mathbf{z}_i$ are normalized. Note that for the last landmark, the x-axis is defined

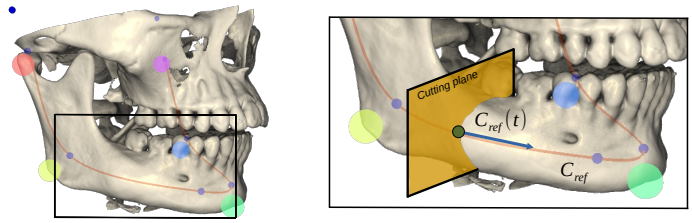

Fig. 2: Mandible reference model $\mathcal{I}_{\text{ref}}$ with its associated reference curves $\mathcal{C}_{\text{ref}}$. Blue spheres represent the control points Φ used to define the curves. The colored spheres represent the anatomical landmarks. Position and orientation of the cutting planes along the curve are defined using the position and tangent at t.

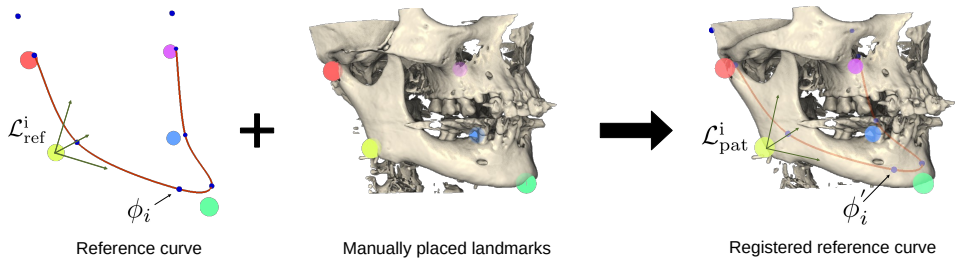

Fig. 3: Reference curve registration process, $\mathcal{C}_{\text{ref}}$ is being deformed onto the patient mandible $\mathcal{I}_{\text{pat}}$ using landmarks placed by the surgeon $\mathcal{L}_{\text{pat}}$.

as $\mathbf{x}_n = \mathcal{L}_{\text{n}} - \mathcal{L}_{\text{n}-1}$. We then perform a non-uniform scaling transformation of the reference model ($\mathcal{L}_{\text{ref}}$ and $\mathcal{C}_{\text{ref}}$) to match the patient's model scale.
After the matching and scaling computation, we compute the transformation matrix T_i that goes from the space of a reference landmark i to the corresponding patient landmark i, such as $T_i = \mathcal{F}_{\text{i}}^{\text{pat}} * \left(\mathcal{F}_{\text{i}}^{\text{ref}}\right)^{-1}$. We use a weighted sum of these transformations to perform the registration of the control points of $\mathcal{C}_{\text{ref}}$ to obtain the patient specific curve $\mathcal{C}_{\text{pat}}$. To do so, we define for each control point a set of weight w_{ij} for each landmark. These weights are based on the inverse of the Euclidean distance between the curve point and the landmark, raised to k a high power to emphasize the influence of nearby landmarks: $w_{ij} = \frac{1}{\left\|\mathcal{L}_{\text{i}}^{\text{ref}} - \phi_j\right\|^k}$. The weights are normalized (the sum of all the control point's weights is equal to 1). We can finally compute each ϕ_j^{pat} as $\phi_j^{pat} = \sum_{i=0}^{n}(w_{ij} * T_i * \phi_i^{ref})$.

2.2 Fibula segmentation

Starting from a lower body CT scan, we generate a fibula mesh, allowing to compute the surgery plan. To do so, the surgeon first selects the chosen fibula (left or right) with a bounding box defined using six sliders (Figure 4 (a)). Then the surgeon places a point on the fibula (Yellow dot on Figure 4 (b)) by clicking on a voxel of a fibula voxel. The rest of the process is automatic. We extract the Z slice of the scan that contains the selected point, we binarize the image and extract all the connected components from the 2D image (green and blue zone in Figure 4 (c)). The tibia is identified as the largest component that does not contain the fibula point (green zone in Figure 4 (c)). We use the identified voxels of tibia, and fibula, as seeds for a watershed algorithm [13], Figure 4 (e), that we perform on the voxels of the bounding box. Having fibula and tibia seeds ensure that the two bones are well separated where they meet. The

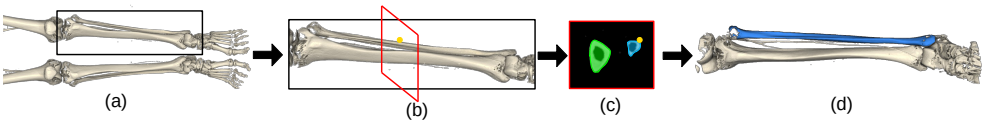

Fig. 4: Fibula segmentation pipeline.

watershed process is stopped just before a peak in the number of voxels corresponding to the fibula. The resulting binary image is used to generate a patient specific surface mesh of the fibula.

2.3 Fibula mesh pretreatment

Once we have the segmented fibula mesh, we define a cutting guide on it. To do so, we first need to obtain a starting point, placed where we can start to extract bone fragments, *i.e.* in the center of the bone at 6cm of the distal part of the fibula (Figure 5 (a)), in order to respect the minimum distance constraint. A vector giving the direction of the fibula (blue arrow on Figure 5), and a vector pointing toward the direction of the pedicle (purple arrow on Figure 5). To obtain those informations, we start by making a Principal Component Analysis (PCA) on the mesh vertices, (green arrows in Figure 5)

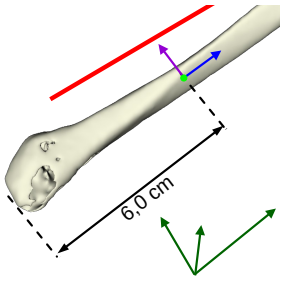

Fig. 5: Fibula pretreatment process

that gives us the main direction of the bone. Giving the known orientation of the patient during the CT scan, and the axis given by the PCA, we then find the most distal vertex of the mesh, and by sliding of 6cm on the main axis of the bone, place the starting point of the cutting trajectory (green point in Figure 5).
To find the direction of the pedicle, we use the same Z slice as the one used to place seeds on the tibia and fibula (Figure 4 (d)), the pedicle direction is set to go from the center of the fibula's component toward the center of the tibia's component. The pedicle is represented by the red line on Figure 5.

2.4 Resections computation

By the nature of the surgery, a deteriorated section of the mandible needs to be removed and subsequently replaced with fibula segments. It is up to the surgeon to decide which section she/he wishes to remove, as well as how many segments of the fibula to use in the reconstruction. The resection computation is performed by giving the control over the two *main* cutting planes P_1 and P_2 defined by $\mathcal{C}_{\text{pat}}(t_1)$ and $\mathcal{C}_{\text{pat}}(t_2)$ (green and red, Figure 1 (d)), where $t_1 < t_2$ and the distance between P_1 and P_2 is greater than d_2 in order to respect the minimum size constraint. For preview reasons, the corresponding planes P_1' and P_2' are placed along the fibula while respecting the prescribed minimum distance by placing P_1' at a distance d_1 from the head of the bone, then P_2' is placed so that the distance between P_1' and P_2' along the curve fibula is equal to the distance between P_1 and P_2 along the mandible curve. The mandible mesh is then cut and the fibula fragments computed.

Fragments positions on the mandible curve The deteriorated section of the mandible between the planes - a curved bone - will need to be replaced with a set of fragments $\mathcal{F}_i$ taken from the fibula - a straight bone. The fragments will be cut at an angle which best imitates the curvature of the patient's jaw. Ideally, the fragments are connected in the mandible at points of high curvature of $\mathcal{C}^{\text{m}}_{\text{pat}}$. Therefore, we

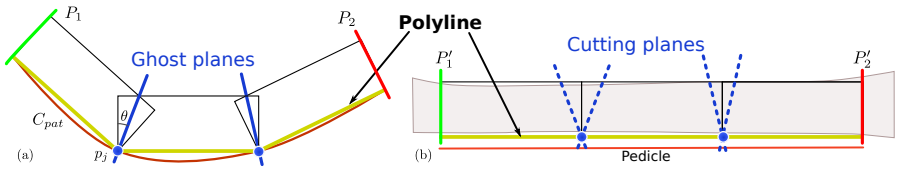

Fig. 6: The polyline structure. (Left) Ghost planes positions (blue), defining polyline points p_j, are maximal curvature points of the mandible curve C_{pat}. Black boxes are placed on the mandible side. (Right) Unfolded polyline (yellow) and boxes (black) onto the mandible curve defining result cutting planes (dotted blue).

place planes within the mandible which represent the connections between the fibula fragments $\mathcal{F}_i$. We note these as *ghost planes*, as illustrated in blue in Figure 6. We use a hill climbing approach to determine the ghost plane positions. We initialize the ghost planes by equally spacing them along the curve. Then we iteratively move each one toward the higher curvature point, while checking that they respect the medical constraints. The curve is smooth enough to prevent the system from falling into local extrema. Sometimes, a prescribed high number of bone fragments makes it impossible to satisfy the minimum size constraint. In this case, we keep the initial step with fragments of equal length. This results in $P = \{p_0, \ldots, p_n\},\ n \leq N$ valid positions for the cutting planes on the mandible, from which we define a structure called the polyline. This is used to compute the cutting planes on the fibula and guarantees that the torsion constraint is respected (Figure 6).

Fibula cutting plane computation We build a piecewise linear curve $C = \bigcup_{j=0}^{t}(p_j,\ p_{j+1})$, and place ghost planes $\mathcal{G}_j$, where $j \in]0, n[$ at each point in $P \backslash \{p_0, p_n\}$. Their orientation δ relative to the pieces of C is defined by the half-angle θ between the two consecutive segments of C at their positions in the mandible. Once all $\mathcal{G}_j$ are created, we build boxes around them, as shown in Figure 6, to place the cutting planes on the fibula. Those boxes will give a first approximation of the fragments $\mathcal{F}_i$. The box are defined as a starting position, a direction, a length, the first plane normal and the last plane normal. So the last plane of a box is the first plane of the next box. C is transferred to the fibula mesh, where it is flattened along its axis (blue arrow in Figure 5). The cutting angles in the fibula are preserved with regard to the fragments which they delimit in the mandible. The boxes representing the fragments $\mathcal{F}_i$ on the fibula are placed on the fibula.

To do so, we define a moving frame along the reference curves without discontinuities in the orientation so as to respect the torsion constraint. Frames defined by Frenet's formulas [14] are usually the go-to choice for moving frames along a curve. However, they can present singularities on points where the curvature changes sign, resulting in 180° rotations along the curve and therefore violating the torsion constraint. To alleviate this issue, we use Bishop frames instead, which are a rotation-minimizing frames [15]. Using it is akin to parallel-transporting a unit normal vector along the curve, and building a frame from that transported vector and the tangent to the curve. The resulting fragments keep the same orientation with minimal torsion of the boxes along $\mathcal{C}^{\mathrm{f}}_{\mathrm{pat}}$. Then the boxes are shifted to leave a precise gap of 1 mm between them.

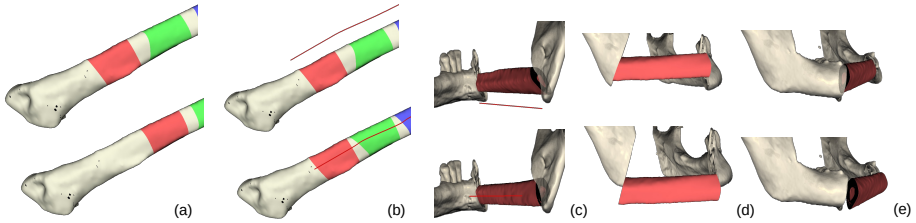

Fig. 7: Manual refinements with sliders.

Cutting planes optimisation To improve the fitting between bones fragments cuts, and thus improve the smoothness of the reconstruction surface, the cutting planes positions and orientations are optimized to maximize the contact between the bones sections. The optimisation process can be viewed as a hill climbing method. Small adjustments are made iteratively to improve the contact between the bone fragments, until no further improvement is observed.

2.5 User refinements

The available manipulators in our software allows the users to express their domain expertise by adjusting the surgery plan. Our manipulators allow adjustments at different scales. The user can choose the global parameter of the surgery, which fibula to use, which way it is grafted and the number of fragments. Then the surgeon can choose the overall shape of the reconstruction with various sliders. Finally, she/he can precisely adjust the placement of the fragments using a set of manipulators.

To adjust the overall shape, we propose the following sliders:

- **Fibula offset** to modify the height at which we start the fragments harvesting on the fibula (Figure 7 (a)).
- **Pedicle position of the fibula** to adjust the position where the pedicle is detected on the fibula. (Figure 7 (b)).
- **Mandible pedicle position** to change the resulting location of the pedicle on the mandible, by rotating the entire reconstruction. (Figure 7 (c)).
- **Reconstruction height** to move the entire reconstruction on the longitudinal axis (Figure 7 (d)).
- **Reconstruction depth** to move the reconstruction toward the inside or the outside of the mandible (Figure 7 (e)).

To adjust precisely the shape of the reconstruction, the surgeon is able to modify the shape of the polyline by moving the points individually. In Figure 8 from (a) to (b), the polyline is modified, and the fragments are recomputed in realtime accordingly. Finally, to give the user the highest level of precision, she/he can adjust the position and orientation of the fragments individually. This does not affect the cutting angles. We can see in Figure 8 from (a) to (c) that the green fragment is rotated, but neither the cutting angles nor the polyline is modified. Note that the visual result (mesh cutting, planes orientation, fragments positioning...) is updated in real-time. During the process, we display a set of metrics, including the gap between the fragments, and

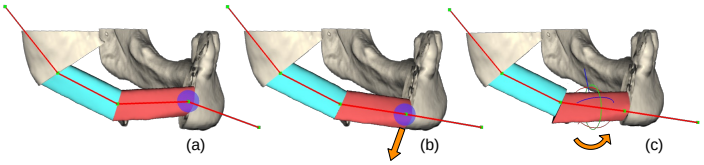

Fig. 8: A polyline manipulation (b) and a fragment manipulation (c), done from an initial configuration (a).

the length of the fragments. However, during the refinements, the surgeon is able to violate the constraints defined earlier, such as the torsion constraints, the minimal bone length or the minimal offset at the bottom of the fibula. This allows the surgeon to handle extreme cases. Once the surgeon is satisfied with the surgical simulation, the coordinates of the cutting planes are transferred to the robot used as a cutting guide during the surgery.

3 Experimental Results

To validate our pipeline, an expert surgeon used our method to compute a surgery plan for two different cases taken from real patient data illustrated Figure 9.

Patient (a) mandible's left body and ramus were reconstructed. The right fibula was used to place the pedicle towards the flap front side, and the skin paddle on the top of the reconstruction. During the manual adjustment, the fibula was rotated to get its lateral cortical side match the lateral cortical side of the mandible, to ease the fixation of the plates.

For patient (b), the front of the mandible was reconstructed. A right fibula was chosen to have the skin paddle on the top of the reconstruction and to anastomose the vessels on the left side of the neck. Manual adjustments took less than 5 minutes in this case, very few modifications were achieved, and only the most distal osteotomy was moved to the back to better fit the mandible curve.

The whole, process starting from raw CT scan data, including segmentation of the fibula in our application, registration of the cutting curve, resection area selection, and manual adjustment, took only from 8 to 13 minutes for each patient where with a commercial solution, such as Materialise, at least a week is necessary from planning to receiving the cutting guides. The surgeon felt that she/he could make exactly what she/he wanted, in a very short time, while having a precise feedback of the final result

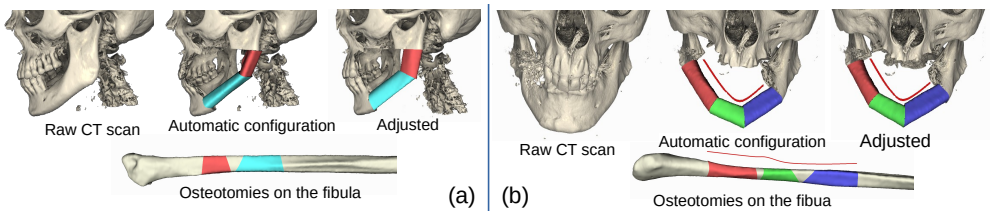

Fig. 9: Automatic and adjusted planning for patient (a) and (b)

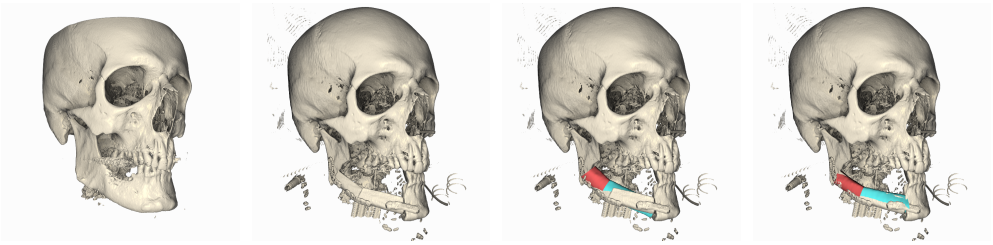

Fig. 10: Comparison between our planning method and Materialise planning.

of the surgery in real time. This highlights the efficiency of our process, the ability of our method to propose accurate automatic reconstructions, and the effectiveness of the manipulators in providing surgeons with a means to apply their expertise.

We validated the curve registration process by applying it to the CT scans of nine patients. For each case, we verified that the curve accurately traverses key anatomical landmarks, including the condyles, ramus, mandibular body, and chin. Additionally, we ensured that the curve remains within the bone structure and is positioned $1cm$ above the inferior edge of the mandible. This placement is critical to ensure that bone fragments are accurately positioned for the next steps of the pipeline.

Our segmentation method relies on a threshold on the values of the CT scan, to discriminate the bone from the background, our specific algorithm aim to extract the fibula from the other bones. The method was validated on both legs of six patient's CT scans. For each of the twelve bones, the surface was accurately segmented, with no inclusion of other bones. Most importantly, the central part of the fibula was segmented with precision, ensuring that its surface is well-defined and detailed.

We measured the medical constraints on nine cases, on the automatic version of the planning, we found that the $7cm$ offset on the distal part of the fibula is respected, the gap between two fibula resection is between $1.01mm$ and $1.50mm$, the small side of the smallest fibula fragments is between 27.87 mm and $41.97mm$ and the twist angle between two consecutive bones fragments is always null (around $1.0e-7^o$). These measures demonstrate that medical constraints are respected.

These experiments (curve registration, automated planning, and medical constraints measurements) are detailed in the supplementary material (Online Resource 1).

We compare our surgery plans to CT scans of three patients who underwent a surgery planned by an expert surgeon the commercial solution propose by Materialise, as illustrated in Figure 10. Our automatic result is close to the performed surgery plan, and after small adjustments on the polyline, we are able to match their planning. After adjustment, on the three cases, the Haussdorf distance between our reconstruction and the post-op scan where $3.8mm$ $4.0mm$ and $4.1mm$. Those distances are below the size of the noise in the post op scan caused by the osteotomies screws, which shows our ability to reproduce the shape of surgeries, planned by an expert. This demonstrates that our method produces automatic planning comparable to a proven commercial

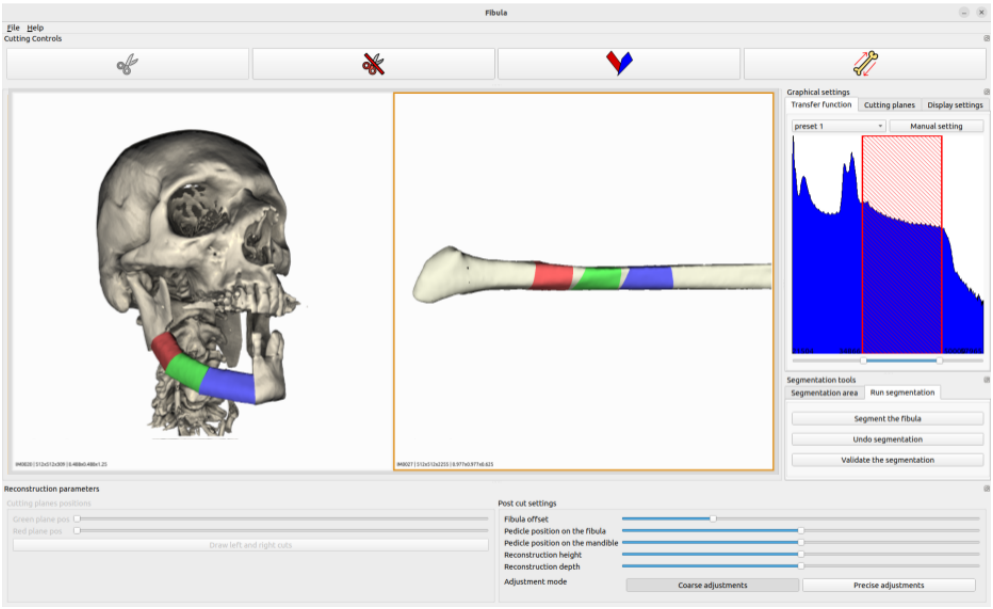

Fig. 11: Graphical User Interface of our application.

solution while allowing the surgeon to achieve the same results with minimal effort. Unlike the commercial software, our approach eliminates the associated costs and delays, as the surgeon does not require direct access to the software, and planning is not instantaneous, often necessitating multiple exchanges with the company. Furthermore, our surgery plan can be directly implemented using robot-assisted surgery, bypassing the additional delays required to produce cutting guides.

Figure 11 shows a snapshot of our Graphical User Interface (GUI) with its two main viewers displaying the mandible CT scan with the fibula resection positioned onto it (left) and the representation of the resection on the fibula (right). Its interactive use is illustrated in the companion video (Online Resource 1).

Our application was tested by three maxillofacial surgeons who completed a satisfaction questionnaire. None of the surgeons had prior experience with computer-based planning but were able to operate the interface autonomously. All three rated the interface's ease of use at 5/5. The interface adaptability received an average score of 4.3/5, while the ability to achieve a realistic planning outcome respecting the FFF constraints an average score of 4.7/5.

We implemented our system in C++, using the *OpenGL* and *Qt* APIs for the user interface and visualization. All our experiments were conducted on a laptop with an Intel i7-8750H processor along with 16GB of RAM and a Nvidia GTX 1070 Max-Q graphics card. The program is interactive for all stages.

4 Discussion and conclusion

In this paper, we proposed an interactive pipeline for mandible reconstruction surgery planning respecting a set of medical constraints increasing the chances of success of the surgery (*i.e.* reducing the risk of graft reject). Using a non-destructive workflow, that takes advantage of the virtual environment afforded by real-time 3D applications, a domain expert is able to generate a realistic surgery plan within minutes that can be intuitively and interactively adjusted if necessary. Our program allows surgeons to design the operation however they see it, and make adjustments as necessary. Our proposed pipeline drastically reduces the delay before the surgery can be performed, is cost-efficient and precise, and is interactive, intuitive, and easy to use by surgeons.

While our method can handle a wide variety of cases, it is currently limited to those where the original shape of the mandible is preserved. This limitation arises because our reconstruction relies on fitting to the healthy parts of the mandible; if these parts have shifted, the resulting reconstruction becomes non-viable. Future improvements could include correcting the mandible's position as a pre-processing step on the skull CT scan and supporting double-barrel reconstructions.

Statements and Declarations

Ethical Statement

Not applicable.

Conflict of Interest Statement

The authors declare that they have no conflict of interest that are relevant to the content of this article.

References

[1] Bak, M., Jacobson, A.S., Buchbinder, D., Urken, M.L.: Contemporary reconstruction of the mandible. Oral oncology **46**(2), 71–76 (2010) https://doi.org/10.1016/j.oraloncology.2009.11.006

[2] Yim, K.K., Wei, F.-C.: Fibula osteoseptocutaneous flap for mandible reconstruction. Microsurgery **15**(4), 245–249 (1994) https://doi.org/10.1002/micr.1920150405

[3] Cohen, A., Laviv, A., Berman, P., Nashef, R., Abu-Tair, J.: Mandibular reconstruction using stereolithographic 3-dimensional printing modeling technology. Oral Surgery, Medicine, Pathology, Radiology, and Endodontology (2009) https://doi.org/10.1016/j.tripleo.2009.05.023

[4] Velasco, I., Vahdani, S., Ramos, H.: Low-cost method for obtaining medical rapid prototyping using desktop 3d printing: a novel technique for mandibular

reconstruction planning. Journal of clinical and experimental dentistry (2017) https://doi.org/10.4317/jced.54055

[5] Chang, E.I., Jenkins, M.P., Patel, S.A., Topham, N.S.: Long-term operative outcomes of preoperative computed tomography–guided virtual surgical planning for osteocutaneous free flap mandible reconstruction. Plastic and reconstructive surgery **137**(2), 619–623 (2016) https://doi.org/10.1097/01.prs.0000475796.61855.a7

[6] Kazhdan, M., Bolitho, M., Hoppe, H.: Poisson surface reconstruction. In: Proceedings of Eurographics Symposium on Geometry Processing (2006). https://dl.acm.org/doi/10.5555/1281957.1281965

[7] Lorensen, W.E., Cline, H.E.: Marching cubes: A high resolution 3d surface construction algorithm. ACM siggraph computer graphics **21**(4), 163–169 (1987) https://doi.org/10.1145/37402.37422

[8] Maisi, S., Dominguez, M., Gilong, P.C., Kiong, C.T., Hajam, S., Badruddin, A.F.A., Siew, H.F., Gopalan, S., Choon, K.T.: In-house virtual surgical planning for mandibular reconstruction with fibula free flap: Case series and literature review. Annals of 3D Printed Medicine **10** (2023) https://doi.org/10.1016/j.stlm.2023.100109

[9] Ritschl, L.M., Kilbertus, P., Grill, F.D., Schwarz, M., Weitz, J., Nieberler, M., Wolff, K.D., Fichter, A.M.: In-house, open-source 3d-software-based, cad/cam-planned mandibular reconstructions in 20 consecutive free fibula flap cases: An explorative cross-sectional study with three-dimensional performance analysis. Frontiers in oncology **11** (2021) https://doi.org/10.3389/fonc.2021.731336

[10] Guo, Y., Xu, W., Tu, P., Han, J., Zhang, C., Liu, J., Chen, X.: Design and implementation of a surgical planning system for robotic assisted mandible reconstruction with fibula free flap. IJCARS **17**(12) (2022) https://doi.org/10.1016/j.ijom.2023.07.010

[11] Cheng, L., Carriere, J., Piwowarczyk, J., Aalto, D., Zemiti, N., Boutray, M., Tavakoli, M.: Admittance-controlled robotic assistant for fibula osteotomies in mandible reconstruction surgery. Advanced Intelligent Systems **3**(1) (2021) https://doi.org/10.1002/aisy.202000158

[12] Twigg, C.: Catmull-rom splines. Computer **41**(6), 4–6 (2003)

[13] Beucher, S., Meyer, F.: The Morphological Approach to Segmentation: The Watershed Transformation, vol. 34, pp. 433–481 (1993). https://doi.org/10.1201/9781482277234-12

[14] Frenet, F.: Sur les courbes a double courbure. Journal de mathématiques pures et appliquées, 437–447 (1852)

[15] Bishop, R.L.: There is more than one way to frame a curve. The American Mathematical Monthly **82**(3), 246–251 (1975) https://doi.org/10.2307/2319846